Ultra-porous superamphiphilic aerogel enabled ultra-stable continuous separation of emulsion

Yujia Wang[a,b], Baicun Hao[a,b], Hanzhong Xiao[b], Yiwen Cui[b], Xin Huang[a,b,*] and Bi Shi [a,b,*]

[a] National Engineering Laboratory for Clean Technology of Leather Manufacture, Sichuan University, Chengdu 610065, P.R. China, xhuangscu@163.com, sibitannin@vip.163.com

[b] College of Biomass Science and Engineering, Sichuan University, Chengdu 610065, P.R. China

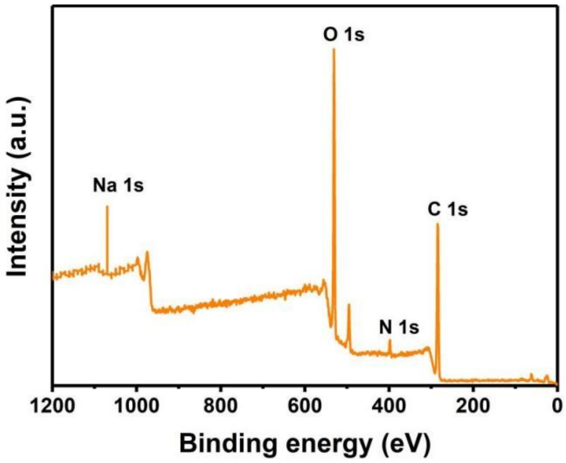

Fig. S1 XPS survey scan spectrum of the CFs-superamphiphilic aerogel.

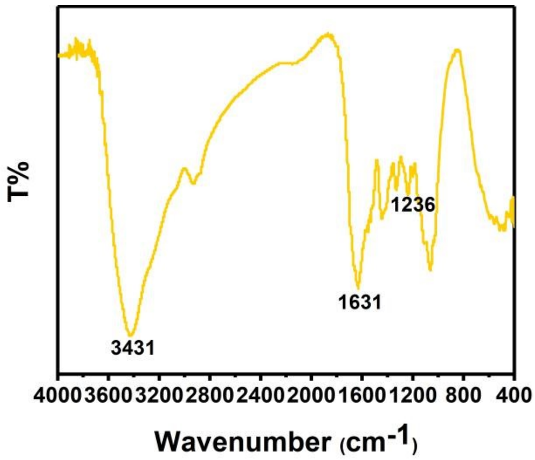

Fig. S2 FTIR spectra of the CFs-superamphiphilic aerogel.

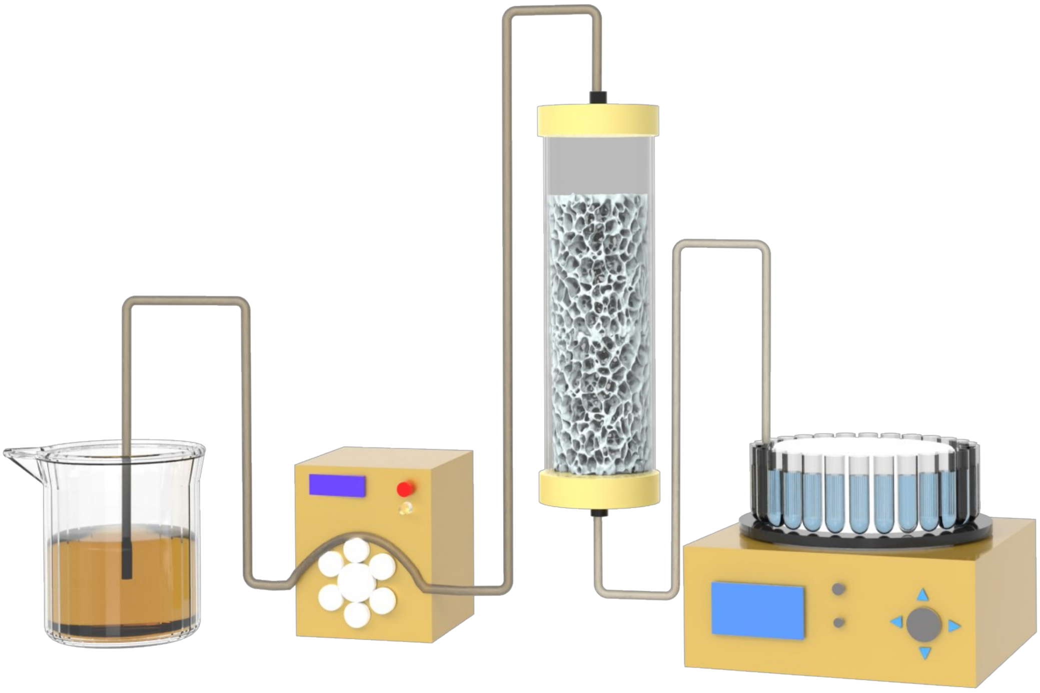

Fig. S3 Schematic illustration showing the emulsion separation system.

Table S1 Ingredients of the prepared W/O emulsions.

Emulsion	Span80 (g)	SDBS/Span80 (g)	CTAB/Span80 (g)	Water (mL)	Dodecane (mL)	Kerosen (mL)	Octane (mL)	Petroleum ether (mL)
NE1	2.0	0	0	8.0	1000	0	0	0
NE2	2.0	0	0	8.0	0	1000	0	0
NE3	2.0	0	0	8.0	0	0	1000	0
NE4	2.0	0	0	8.0	0	0	0	1000
NE5	0	0.1 /1.5	0	10.0	1000	0	0	0
NE6	0	0.1 /1.5	0	10.0	0	1000	0	0
NE7	0	0.1 /1.5	0	10.0	0	0	1000	0
NE8	0	0.1 /1.5	0	10.0	0	0	0	1000
NE9	0	0	0.1 /1.5	10.0	1000	0	0	0
NE10	0	0	0.1 /1.5	10.0	0	1000	0	0
NE11	0	0	0.1 /1.5	10.0	0	0	1000	0
NE12	0	0	0.1 /1.5	10.0	0	0	0	1000

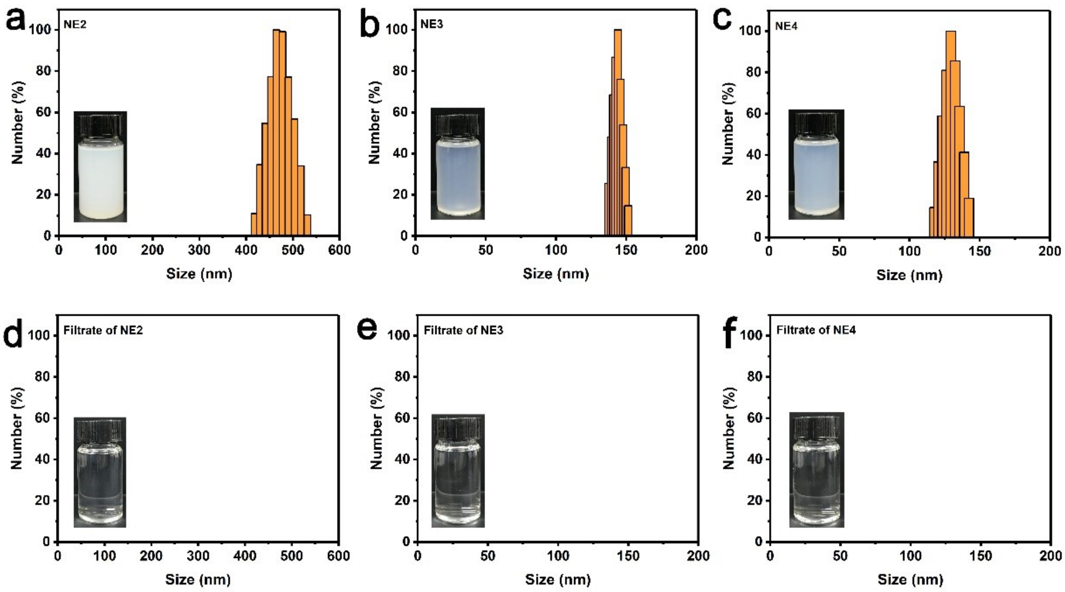

Fig. S4 DLS curves of NE2 (a) before and (d) after the separation by the CFs-superamphiphilic aerogel, DLS curves of NE3 (b) before and (e) after the separation by the CFs-superamphiphilic aerogel, DLS curves of NE4 (c) before and (f) after the separation by the CFs-superamphiphilic aerogel. The insets in a and d show the digital photographs of NE2 and the filtrate of NE2, respectively. The insets in b and e show the digital photographs of NE3 and the filtrate of NE3, respectively. The insets in c and f show the digital photographs of NE4 and the filtrate of NE4, respectively.

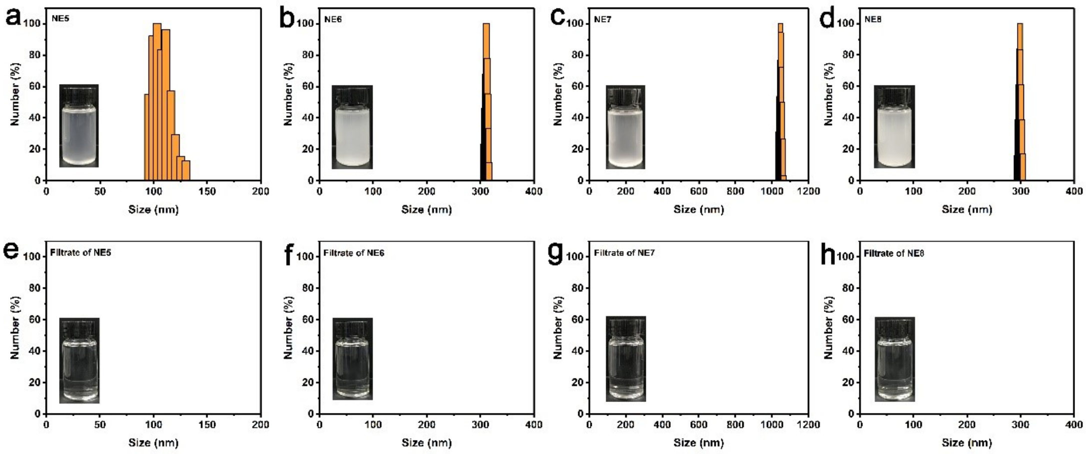

Fig. S5 DLS curves of NE5 (a) before and (e) after the separation by the CFs-superamphiphilic aerogel, DLS curves of NE6 (b) before and (f) after the separation by the CFs-superamphiphilic aerogel, DLS curves of NE7 (c) before and (g) after the separation by the CFs-superamphiphilic aerogel, DLS curves of NE8 (d) before and (h) after the separation by the CFs-superamphiphilic aerogel. The insets in a and e show the digital photographs of NE5 and the filtrate of NE5, respectively. The insets in b and f show the digital photographs of NE6 and the filtrate of NE6, respectively. The insets in c and g show the digital photographs of NE7 and the filtrate of NE7, respectively. The insets in d and g show the digital photographs of NE8 and the filtrate of NE8, respectively.

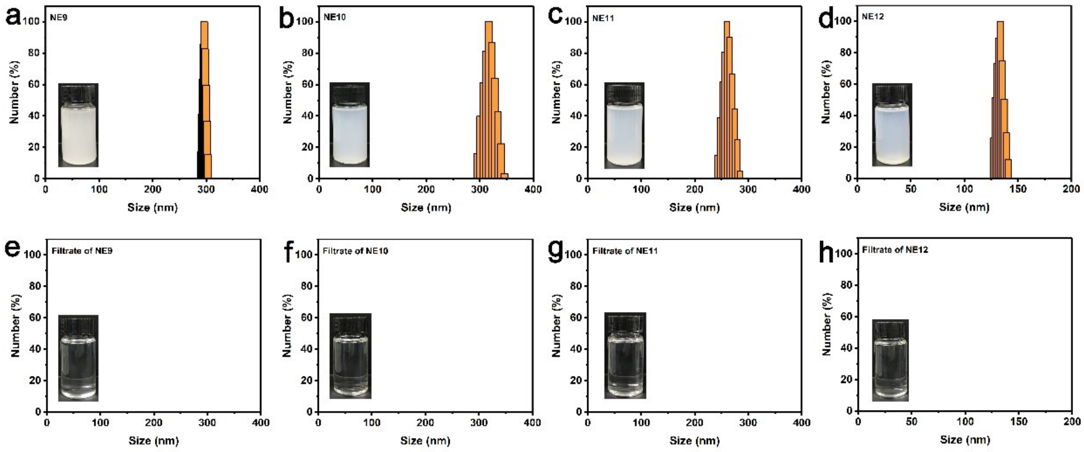

Fig. S6 DLS curves of NE9 (a) before and (e) after the separation by the CFs-superamphiphilic aerogel, DLS curves of NE10 (b) before and (f) after the separation by the CFs-superamphiphilic aerogel, DLS curves of NE11 (c) before and (g) after the separation by the CFs-superamphiphilic aerogel, DLS curves of NE12 (d) before and (h) after the separation by the CFs-superamphiphilic aerogel. The insets in a and e show the digital photographs of NE9 and the filtrate of NE9, respectively. The insets in b and f show the digital photographs of NE10 and the filtrate of NE10, respectively. The insets in c and g show the digital photographs of NE11 and the filtrate of NE11, respectively. The insets in d and h show the digital photographs of NE12 and the filtrate of NE12, respectively.

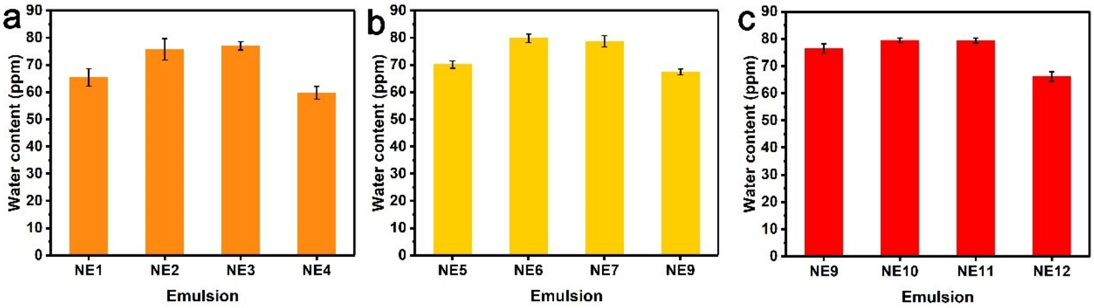

Fig. S7 (a) Water contents in the filtrates of NE1, NE2, NE3 and NE4 separated by the CFs-superamphiphilic aerogel, (b) water contents in the filtrates of NE5, NE6, NE7 and NE8 separated by the CFs-superamphiphilic aerogel, (c) water contents in the filtrates of NE9, NE10, NE11 and NE12 separated by the CFs-superamphiphilic aerogel.

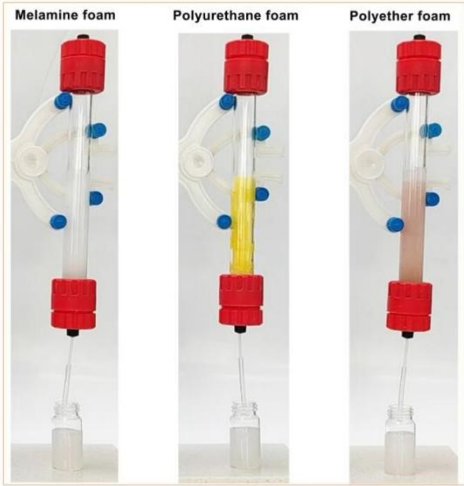

Fig. S8 Images showing the separation failure of NE1 by melamine foam, polyurethane foam and polyether foam, respectively.